ISSUE: November 2024

Designing An Open-Source Power Inverter (Part 21): Converter Inductor Winding Design

by Dennis Feucht, Innovatia Laboratories, Cayo, Belize

As this series[1-20] moves forward, we explore the Volksinverter's battery converter stage further, continuing the design of the inductor of the boost push-pull (BPP) transfer circuit. A two-winding coupled inductor as shown in Fig. 1, the Volksinverter boost or common-active (CA) PWM-switch inductor is the only power-transfer component (along with the fuse and connectors) that is in series with the battery and conducts the most current of all the Volksinverter circuitry.

The procedure for magnetic component design begins logically with the magnetic design—the design associated with the core—for without it, there is nothing on which to base the winding (electrical) design. The previous article in this series (part 20) presented the magnetic design from which we have Table 1, repeated here. Inductor core types are under the "L Core" column. Minimum inductance L_{min} is needed for current protection, L_{max} is the maximum inductance and energy storage (or transfer power) value at I_{gmax} and N_{max}, and N_w is the maximum turns that fit the core window.

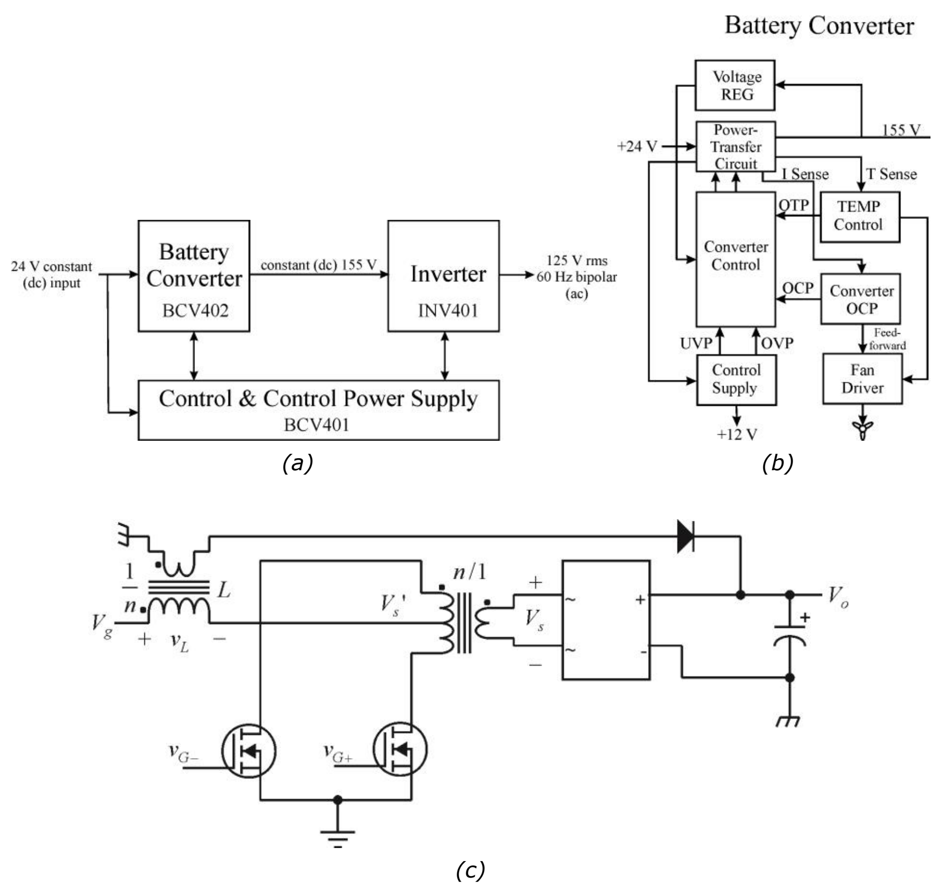

Fig. 1. The Volksinverter's system block diagram (a), the BCV402 battery converter stage block diagram (b) and the extended BPP power-transfer circuit that operates in both CA (boost) and CP (buck) modes (c). In this power-transfer circuit, turns ratio n determines V_s' and hence v_L during off-time. The focus of this part is the design of the two-winding couped inductor L.

Table 1. Four BCV402 transformer cores and their inductance parameters.

xfmr core	$\overline{P}_g$, W	$\overline{P}_{Ld}$, W	$I_{g\max}$, A	**L core**	l, cm	L_0, µH	N_w	$N_{\max}$	N_λ	N_{opt}	$L_{\max}$, µH	$L_{\min}$, µH
ETD34	333	167	16.67	**2 T130**	8.28	127	62	62	13	28	114	3.3
ETD39	436	218	21.8	**2 T131**	7.72	112	35	44	11	22	57.8	2.5
ETD39	436	218	21.8	**E162**	8.41	121	21	48	12	24	68.6	2.5
EER40	511	256	25.6	**2 T150**	9.38	92.9	49	45	11	22	62.1	2.2
EER42	613	307	30.7	**2 T157**	10.1	72.2	49	41	9	19	50.0	1.8

Note: inductor core material: Micrometals 26

Inductor winding design of the first Table 1 entry is presented here. Other entries would follow the same basic procedure.

Magnetic Design Summary

The 2 × T130-26 parameters from the circuit and magnetic design (part 19) or the Micrometals core catalog are

Full-scale operating-point: max I_L = 16.67 A @ V_g = 20 V, $D = D'$ = 0.5

$2\cdot\mathcal{L}_0 = 2\cdot 81$ nH = 162 nH; A_w = 308 mm²; A_{wp}' = 160 mm²; A_{ws}' = 71.2 mm²; ID = 19.8 mm ⇒ r_i = 9.90 mm

$\overline{p}_c$ = (1.8)·(160 mW/cm³) = 287 mW/cm³ ⇒ from core-loss graph, $\hat{B}_\sim(\overline{p}_c) = 20$ mT ⇒ triangle-wave $\hat{B}_\sim(\overline{p}_c) \approx$ 18 mT

$$\overline{P}_c = (287\,\text{mW/cm}^3)\cdot(11.56\,\text{cm}^3) = 3.32\text{ W} \Rightarrow \text{min-}P_t\text{, max-}\eta \Rightarrow \overline{P}_w \approx \overline{P}_c \Rightarrow$$

$$R_{wpopt} = \frac{\overline{P}_c}{\tilde{i}_L^{\,2}} \approx \frac{3.32\text{ W/2}}{\tilde{i}_L^{\,2}} = \frac{1.66\text{ W}}{(16.67\text{ A})^2} = 5.97\,\text{m}\Omega \approx 6\,\text{m}\Omega$$

= 12 mΩ || 12 mΩ, power-circuit model of push-pull primary windings

$$N_p \ge N_\lambda = \frac{\Delta\lambda_{\max}}{\Delta\phi(\overline{p}_c)} = \frac{(V_s' - V_g)\cdot[D_{\max}'\cdot T_s]}{[2\cdot\hat{B}_\sim]\cdot(2\cdot A)} = \frac{(20\text{ V})\cdot[(0.5)\cdot(6.67\,\mu\text{s})]}{2\cdot(18\text{ mT})\cdot(1.4\text{ cm}^2)} = \frac{66.7\,\mu\text{V}\cdot\text{s}}{5.04\,\mu\text{V}\cdot\text{s}} = 13.23 \approx 13$$

$$L_0 = N_p^{\,2}\cdot\mathcal{L}_0 \ge 28^2\cdot 162\text{ nH} = 127\,\mu\text{H} > L_{\min} = 3.3\,\mu\text{H}$$

$$\text{Secondary current (full-scale)} = \tilde{i}_s(\max) \approx 1.70\text{ A}$$

For the secondary winding, a #21 AWG wire has the ampacity of $I_{\max}$ = 1.88 A > $\tilde{i}_s(\max)$, and one AWG wire size smaller, or #22, can sustain 1.492 A. $\tilde{i}_s(\max)$ straddles the two sizes, and either size is a possible choice, though #21 provides a greater design margin if it fits the winding area; #21 exceeds somewhat the ampacity requirement.

Whether #22 ampacity is acceptable is assessed by the designer based on the importance of reliability in the application. If it pushes too far beyond the margin, either the T130 core might be replaced with a T150 that has a larger window area or turns are reduced to fit the allotted areas.

Winding Design

By setting $N_{opt} = N_\lambda = N_i = N_{\max} \le N_w$, maximum power density is achieved in the core. Above $N_i = N_{\max}$, core energy and inductance are reduced; $N_{\max}$ sets an upper bound on saturation. Except for the E162 Table 1 entry $N_{\max} \le N_w$, but even then, to wind toroids, a center area must be kept open to pass turns through. Optimal N is achieved by setting margins between N_λ and N_i that allow the core to be driven to both a maximum $\Delta\lambda$ and I simultaneously;

$$N_{opt} = \sqrt{N_\lambda \cdot N_i} = \sqrt{N_\lambda \cdot N_{\max}}\ ,\ N_\lambda = (18.52\ \text{cm}^2)/A$$

With fewer turns, core energy density is less than what it would be at $N_{\max}$. However, $N_{\max}$ would place the magnetic operating-point at the greatest saturation beyond which inductance and energy storage decrease quickly. Although $N_{\max}$ offers greatest ΔW_L, L, and minimum Δi, it teeters on the edge of oversaturation. Consequently, if the op-pt is backed away from $N_{\max}$ by the same margin as from N_λ, N_{opt} becomes the choice.

Another alternative, reminiscent of transformer design, is to fill the allotted winding areas with as many turns as will fit. This is the default criterion whenever $N_{opt} > N_w$ (or N_p or N_s), and operation moves closer to core overheating than oversaturation.

Primary Winding

To wind a toroid, some center space is needed through which to thread the bundle turns. An allotment of a central 25% of open window area for threading leaves 75% for windings. Half of the toroid window radius r_i remains open at the center to $r_i/2$. Then maximum winding area fraction $k_{ww} \leq 0.75$.[2 22] The available primary winding area is

$$A_{wp}' = k_{ww} \cdot A_w = A_w' - A_{ws}' = (308\ \text{mm}^2)\cdot(0.75) - 71\ \text{mm}^2 = 160\ \text{mm}^2$$

The primary winding turns is

$$N_p = N_{opt} = \sqrt{N_\lambda \cdot N_{\max}} = \sqrt{(13)\cdot(62)} = 28.4 \rightarrow 28$$

It is allotted A_{wp}' of winding area with an area per turn of

$$\text{pri}\ \ A_{bwp} = \frac{A_{wp}'}{N_p} = (160\ \text{mm}^2)/28 = 5.71\ \text{mm}^2$$

This is the *packed insulated bundle* area, including conductor and surrounding non-conductor, attributed to each turn.

A wire or bundle turn has a radius from which the area of the turn itself can be found as $A_{bw} = \pi \cdot r_{bw}'^2 < A_{bwp}$. The area required by a winding with turns N of r_{bw}' radius is more than $N \cdot A_{bw}$ because of the non-conductive space surrounding each turn that is unavoidable because of how turns pack together in layers. This wasted space is included in the *packing factor* k_p, the product of particular packing factors.

By definition, for a given winding area, k_p is the fraction of area within it that is conductor. *Porosity* k_{pw}, the fraction of area lost to spacing from wire insulation or turns separation, and bundle *twist factor* k_{tw} are typically smaller that the dominant *fill factor* k_{pf} attributed to nonconductive spaces formed within layers of round turns. Strands within a bundle have a fill factor of k_{pb}. Wire porosity, bundle fill factor, and bundle twist apply to the bundle while the fill factor of winding turns k_{pf} applies to the winding. Thus,

$$k_p = (k_{pf}) \cdot (k_{tw} \cdot k_{pw} \cdot k_{pb})$$

As the fraction of conductor area, k_p relates to the wire conductive radius r_c. If the insulated wire radius r_{cw} is of interest instead, k_{pw} is omitted because it is included in the larger r_{cw} over r_c. (Other spacing than insulation between wires can cause k_{pw} to be larger.) The bundle radius formula is r_{bw}'/r_{cw} and is based on insulated strand radius r_{cw}. Thus k_{pw} does not appear in the formula for the ratio. Consequently, the twisted bundle radius, with bundle fill and twist factors included, is

$$\text{pri } r_{bw}' = \sqrt{\frac{A_{bwp} \cdot k_p}{\pi}} \approx \sqrt{\frac{A_{bwp} \cdot k_{pb} \cdot k_{tw}}{\pi}} = 1.182 \text{ mm}, \; k_{pb} = k_{pf} = \pi/4 \approx 0.7854, \; k_{tw} = 1/1.022 = 0.9785, \; k_p = 0.7685$$

where $A_{bwp} \cdot k_p$ is the insulated bundle area and k_{tw} is bundle expansion for a twist tightness of $p/r_{bw}' = 30$. Porosity k_{pw} is already included in A_{bwp} because it is based on insulated strand radius r_{cw}, not conductive radius r_c.

In calculating the maximum bundle radius that fits the allotted winding area, this radius is for the twisted (′) insulated bundle itself and has within it the bundle fill and porosity factors. Porosity is included in the bundle radius to be calculated as the radius insulated by bundle strands, including possibly wrapped insulating tape. Assume that strands within the bundle have the same fill configuration (square or hexagonal) as bundles in the winding ($k_{pb} = k_{pf}$) because both have the same round shape and packing pattern. The winding fill factor k_{pf} is *interbundle* while $k_{pw} \cdot k_{pb}$ are contained within r_{bw}'. The bundle of N_s strands, however configured internally, is constrained to this radius.

Around the toroid is 28 contiguous turns of total primary-winding "layer width"

$$w_p = N_p \cdot (2 \cdot r_{bw}') = 28 \cdot [(2) \cdot (1.182 \text{ mm})] = 28 \cdot (2.364 \text{ mm}) = 66.19 \text{ mm}$$

Adjacent turns along the toroid core inside diameter (ID) form a layer with first-layer circumferential "width" of

$$\text{First-layer circumference} = w_{p1} = 2 \cdot \pi \cdot (r_i - r_{bw}') = 2 \cdot \pi \cdot (9.90 \text{ mm} - 1.182 \text{ mm}) = 54.78 \text{ mm}$$

The primary turns that fit the first layer are

$$N_{lp1} = \frac{2 \cdot \pi \cdot (r_i - r_{bw}')}{2 \cdot r_{bw}'} = \pi \cdot \left(\frac{r_i}{r_{bw}'} - 1 \right) = 23.17 \rightarrow 23$$

The primary winding fills more than the first layer;

$$M_{p1} = w_p / N_{lp1} = 66.19 \text{ mm}/54.78 \text{ mm} \approx 1.21 \text{ layers} > 1 \text{ layer}$$

Toroid layers have decreasing turns/layer N_l with increasing layers. Consequently, the second layer has an available circumference (assuming a worst-case square packing of layers) of

$$\text{Second-layer circumference} = 2 \cdot \pi \cdot (r_i - 3 \cdot r_{bw}') = 2 \cdot \pi \cdot (9.90 \text{ mm} - 3.546 \text{ mm}) = 2 \cdot \pi \cdot (6.354 \text{ mm}) = 39.92 \text{ mm}$$

The remaining 28 – 23 = 5 turns require a width of

$$w_{p2} = 5 \cdot (2.364 \text{ mm}) = 11.82 \text{ mm}$$

and fill 11.82 mm/39.92 mm = 0.296 or about 30% of the second layer. Hence

$$M_p = 1.30$$

As a numeric check, total width w_p should be the sum of the widths of the two layers, or

$$w_{p1} + w_{p2} = 54.78 \text{ mm} + 11.82 \text{ mm} = 66.6 \text{ mm} \approx w_p = 66.2 \text{ mm}$$

The result is not exact because N_{lp1} is rounded down to 23, resulting in second-layer turns of 5 instead of 4.83.

Some additional winding area is lost because winding bundles do not conform perfectly to the sides of the core stack and consequently, layer "bowing" along the stack height loses some area. Primary bundles leave fill spaces between turns for the smaller secondary windings to occupy, but most of it is lost because insulating tape between primary and secondary windings partially blocks crevices between primary turns that secondary wire could occupy. Three layers of 1-mil = 25.4-μm polyester tape has a thickness of 76.2 μm = 0.076 mm—an almost negligible area.

Bundle Design of Primary Winding

The primary winding design goals are to minimize eddy-current resistance and support an average of 16.67 A. Eddy-current loss is reduced and bundle packing maximized in a bundle with three strands, resulting in a minimal r_{bw}'. A strand size of sufficient strand ampacity requires

$$I_{\max} \geq I_{g\max}/N_{s0} = (16.67 \text{ A})/3 = 5.56 \text{ A} \Rightarrow (5.56 \text{ A})/(0.833) = 6.67 \text{ A} \Rightarrow \#\,15 \Rightarrow I_{\max} = 7.52 \text{ A},\ r_{cw} = 0.781 \text{ mm}$$

where $\tilde{J}/\tilde{J}_0$ = 0.833 for a 2 × T130 core. Core size adjustment of the thermal winding model requires that the specified current be ×1.2 larger. The total primary strands in the winding area are

$$N_s \cdot N_p = 3 \cdot 28 = 84$$

The twisted bundle radius to strand-radius ratio = r_{bw}'/r_{cw} is a function of strands N_s. The twisted bundle radius per strand radius for N_s strands is given in Table 2.

Bundle radius is derived from strand radius N_s and bundle packing factor k_{pb};

$$\frac{r_{bw}'}{r_{cw}} = \sqrt{\frac{N_s}{k_{pb} \cdot k_{tw}}} = 1.886,\ \ k_{tw} = 0.9788,\ p/r_{bw} = 30,\ p = \text{twist pitch (length of twist cycle)} \Rightarrow$$

$$r_{bw}' = (0.781 \text{ mm}) \cdot (1.886) = 1.473 \text{ mm}$$

Table 2. Bundle radius for N_s strands, untwisted ($1/k_{pb}$) and twisted (r_{bw}'/r_{cw}).

N_s	$1/k_{pb}$, $p \to \infty$	$\frac{r_{bw}'}{r_{cw}}$
2	2 max, 1.55 avg	2.022
3	**1.16 max, 1.13 avg**	**1.886**
4	1.662 avg	2.605
5	1.37 avg	2.646
6	1.265	2.785
7	1.286	3.033
8	1.742	3.773

Note: twisted p/r_{bw} = 30

Then the primary winding of N_p bundle turns occupies an area of

$$A_{wp} = N_p \cdot A_{bw}' = N_p \cdot (\pi \cdot r_{bw}'^2) = 28 \cdot \pi \cdot (1.473 \text{ mm})^2 = 191 \text{ mm}^2 < A_{wp}' = 206 \text{ mm}^2$$

The primary winding fits well its allotted area as a twisted bundle of 3 × #15 wire occupying 191/206 = 0.927 of A_{wp}'.

A secondary winding of #22 wire has I_{max} = 1.492 A, within one integer AWG of the specified 1.7 A. Then 112 turns of #22 wire have an area of $N_s \cdot A_{cwp}$ = (112)·(0.510 mm^2) = 57.1 mm^2 > 53.4 mm^2. The allotted area is exceeded by (57.1 – 53.4) mm^2 = 3.7 mm^2 but the extra area from the primary winding is (206 – 191) mm^2 = 15 mm^2, leaving a total area in excess of about 11 mm^2.

Secondary Winding

Proceeding in the same way for a sequential secondary winding, the available secondary winding area is

$$A_{ws}' = (71.2 \text{ mm}^2) \cdot (0.75) = 53.4 \text{ mm}^2$$

The secondary winding has

$$N_{Ls} = (1/n) \cdot N_p = 4 \cdot 28 = 112 \text{ turns}$$

and is allotted A_{ws}' of winding area. As a single strand, it has a maximum packed size of

$$\sec\ A_{cwp} = \frac{A_{ws}'}{(1/n) \cdot N_p} = (53.4 \text{ mm}^2)/(112) = 0.477 \text{ mm}^2$$

As a single-strand winding it has a radius of

$$\sec\ r_{cw}' = \sqrt{\frac{A_{cwp} \cdot k_p}{\pi}} \approx \sqrt{\frac{A_{cwp} \cdot k_{pb} \cdot k_{tw}}{\pi}} = 0.3416 \text{ mm},\ k_{pb} = k_{pf} = \pi/4 \approx 0.7854,\ k_{tw} = 1/1.022 = 0.9785,\ k_p = 0.7685$$

Because the primary winding fills only 30% of its second layer, the remaining 60% can be filled by secondary turns. The secondary winding is wound over 60% of the primary winding first layer and over 30% of the second layer. The primary winding has M_p = 1.3 layers and r_{bw}'(pri) = 1.182 mm, which leaves an average secondary radius of

$$r_{is} = r_i - \{2 \cdot r_{bw}'(\text{pri}) + (M_p - 1) \cdot [4 \cdot r_{bw}'(\text{pri})]\} = r_i - \{(2 \cdot M_p - 1) \cdot 2 \cdot r_{bw}'(\text{pri})\}$$

$$= 9.90 \text{ mm} - \{(1.6) \cdot (2.364 \text{ mm})\} = 6.118 \text{ mm}$$

Adjacent turns along the first layer of the secondary winding fill a layer width of

$$\text{First-layer circumference} = w_{s1} = 2 \cdot \pi \cdot (r_{is} - r_{bw}') = 2 \cdot \pi \cdot (6.118 \text{ mm} - 0.3416 \text{ mm}) = 2 \cdot \pi \cdot (5.776) = 36.29 \text{ mm}$$

The turns that fit the secondary first layer are

$$N_{ls1} = \pi \cdot \left(\frac{r_{is}}{r_{cw}'} - 1 \right) = 53.12 \rightarrow 53$$

The total secondary winding "layer width" is

$$w_s = N_{Ls}\cdot(2\cdot r_{bw}') = 112\cdot[(2)\cdot(0.3416\text{ mm})] = 112\cdot(0.6832\text{ mm}) = 76.52\text{ mm}$$

$$\text{Second-layer circumference} = 2\cdot\pi\cdot(r_{is} - 3\cdot r_{cw}') = 2\cdot\pi\cdot(6.118\text{ mm} - 1.025\text{ mm}) = 2\cdot\pi\cdot(5.093\text{ mm}) = 32.00\text{ mm}$$

The remaining second-layer turns of 112 – 53 = 59 spread across a width of

$$w_{s2} = 59\cdot(0.6832\text{ mm}) = 40.31\text{ mm} \Rightarrow 40.31\text{ mm}/76.52\text{ mm} = 0.527\text{ layers}$$

As a numeric check, total width w_s should be the sum of the widths of the two layers, or

$$w_{s1} + w_{s2} = 36.29\text{ mm} + 40.31\text{ mm} = 76.6\text{ mm} \approx w_p = 76.52\text{ mm}$$

The result is not exact because N_{ls1} is rounded down to 53, resulting in second-layer turns of 59 instead of 58.88.

The secondary winding design is not completed unless the wire size and length are also specified. The insulated wire radius is $r_{bw}' = 0.3416$ mm which is found on the wire table between #23 and #22 AWG but closer to #22. Another way to size the wire is by finding $A_{cwp} = 0.477\text{ mm}^2$ on the wire table, and it also occurs between #23 and #22.

The required ampacity of the secondary winding from the specification is 1.7 A, though this is based on the assumption that CP and CA modes would have the same duration in overcurrent. Wire size #21 has ampacity $I_{max} = 1.88$ A > 1.7 A and meets the specification. As one size smaller, #22 is a possible choice, at $I_{max} = 1.492$ A, though it is a decision of how much design margin is acceptable.

Multifilar Winding Configuration

For toroids, the winding lengths also must be known before cutting wire. Although it is possible to derive design equations for sequentially-wound windings geometrically, as we have been doing, a simpler way to fill the allotted winding areas is to configure windings differently. This does not alleviate the need to find winding lengths, but a different configuration of windings—the unibundle—also solves the length problem, making primary and secondary strands the same length.

We have assumed a sequential winding configuration but a multifilar (parallel) alternative is feasible if the secondary winding wire is wrapped with insulation tape, multifilar-wound with three strands of #15 wire of the primary. An additional simplification can be made by designing the bundle with only one strand size—that of #22 wire. Then to sustain the required primary ampacity, the primary requires

$$I_g / I_{max}(\#22) = 16.67\text{ A}/1.492\text{ A} = 11.17 \rightarrow 11\text{ strands of \#22 wire}$$

Four secondary strands connect in series for the required secondary turns. Then the bundle radius for 15 #22 strands layered in a hexagonal configuration within the bundle (so that $k_{pb} = \pi/4 \approx 0.7854$) and twisted with $k_{tw} = 0.979$, is

$$r_{bw}' = r_{cw}\cdot\sqrt{\frac{N_s}{k_{pb}\cdot k_{tw}}} = (0.359\text{ mm})\cdot\sqrt{\frac{15}{0.769}} = (0.359\text{ mm})\cdot(4.417) = 1.586\text{ mm}$$

The total unibundle width is

$$w_b = 28\cdot(2)\cdot(1.586\text{ mm}) = 88.82\text{ mm}$$

The unibundle fills the available layer width for the first layer;

$$\text{First-layer circumference} = w_1 = 2\cdot\pi\cdot(r_i - r_{bw}') = 2\cdot\pi\cdot(9.9\text{ mm} - 1.586\text{ mm}) = 2\cdot\pi\cdot(8.314\text{ mm}) = 52.24\text{ mm}$$

The turns for a full first layer are

$$N_{l1} = \pi\cdot\left(\frac{r_i}{r_{bw}'} - 1\right) = 16.47 \rightarrow 16$$

The remaining winding width is (88.82 – 52.24) mm = 36.58 mm. The available second-layer width is

$$\text{Second-layer circumference} = w_2 = 2\cdot\pi\cdot(r_i - 3\cdot r_{bw}') = 2\cdot\pi\cdot(9.9\text{ mm} - 3\cdot 1.586\text{ mm}) = 2\cdot\pi\cdot(5.142\text{ mm}) = 32.31\text{ mm}$$

The turns for a full second layer are

$$N_{l1} = \pi\cdot\left(\frac{r_i}{r_{bw}'} - 3\right) = 10.185 \rightarrow 10$$

What remains to be wound is

$$w_b - (w_1 + w_2) = 4.27\text{ mm}$$

This is 1.35 bundle diameters and for the third layer consists of the remaining 28 – (16 + 10) = 2 turns through the core center.

The total available winding area is A_w' = 231 mm^2. The total area of 28 bundle turns is

$$(28)\cdot\pi\cdot(1.586\text{ mm})^2/k_{pf} = 221\text{ mm}^2 < A_w' = 231\text{ mm}^2$$

The bundle diameter is $2\cdot r_{bw}'$ = 3.155 mm.

This *unibundle* fits the allotted winding area. It is the easiest to construct, uses one wire size, but requires more pins for the secondary series connections. The induced voltage is the same across all strands along their lengths, though the static voltage increases across series strands. Electrical isolation is achieved by resorting to a *duobundle*, a bundle for each winding: four twisted strands of #22 wire wrapped in tape, and 11 twisted strands of #22 for the primary winding. For higher coupling, the two bundles can be twisted into a single bundle, though packing is reduced which might require a reduction in wire size to fit the winding area.

The unibundle configuration might be acceptable if heavy (double-insulated enamel) wire (which has been assumed all along) is used, though wrapping the secondary strands together with tape before twisting the bundle minimizes lost area, maximizes coupling, and minimizes eddy-current resistance. Thus, it will be selected for the remainder of the inductor winding design.

Winding Length

We need unibundle winding length to not only cut wire for bundle construction but also to calculate eddy-current resistance. Calculate winding length l_w and twisted length l_w' based on the T130 geometric parameters:

$$\text{T130: } r_i = 9.9\text{ mm};\ w = 6.6\text{ mm};\ h = 11.1\text{ mm};\ \text{stacked: } 2\cdot h = 22.2\text{ mm};\ 2\cdot(h + w) = 28.8\text{ mm};\ r_i + w/2 = 13.2\text{ mm}$$

The toroid winding length design formulas are taken from references [23]or [24]. For the unibundle, substitute $N \leftarrow N_b = 28$, $r_{cw} \leftarrow r_{bw}' = 1.586$ mm

Maximum layers = $\hat{M} = \dfrac{r_i}{(1.866)\cdot r_{cw}}$ = 3.363

$N_w = \pi \cdot \hat{M}^2$ = 35.53

$M = \hat{M} \cdot \left(1 - \sqrt{1 - \dfrac{N}{N_w}}\right)$ = 1.815

$$l_w = 2\cdot\pi\cdot M \cdot [(2\cdot(h+w)+8\cdot r_{cw}\cdot M)\cdot(\hat{M} - M/2) + \tfrac{4}{3}\cdot r_{cw}\cdot(1-M^2) + (r_i + w/2)]$$

= (11.40)·[(28.8 mm + 22.90 mm)·(2.456) – 4.824 mm + 13.2 mm)]

= (11.40)·[127 mm – 4.824 mm + 13.2 mm] (11.40)·[135.4 mm] = 154 cm

Add twisting effect on length:

$l_w' = l_w/k_{tw} = l_w/0.9788$ = 157.6 cm

Add about 3 cm to each end for termination. Then

l_w = 164 cm

Eddy-Current Effects

Eddy-current strand and proximity effects are negligible for twisted strands of $N_s \le 5$, leaving only strand (f_{rS}) and bundle (f_{rB}) skin effects.[25] The bundle skin effect resistance ratio is

$$f_r = \frac{F_r}{N_s} = \frac{f_{rS}}{N_s} + f_{rB}$$

In a unibundle, there are opposing currents in primary and secondary strands, and this both reduces eddy-current resistance and complicates the analysis somewhat.

From the eddy-current F_r plots of Fig. 2, where the lowest plot, designated $F_R/\xi_r^2 = f_{rS}$. Then the primary winding

$$f_{rS}(\#22) = 0.415/11 = 0.038$$

To find f_{rB}, the bundle radius

$$r_{bw}' = 1.5776\text{ mm} \rightarrow \#9 \Rightarrow f_{rB}(\#9) \approx 0.070 \Rightarrow f_r = 0.415/11 + 0.070 = 0.108 \Rightarrow$$

$$R_w = f_r \cdot \left[\left(\frac{R_{\delta r}}{l_w}\right)\cdot l_w'\right] = f_r \cdot \frac{R_{\delta r}}{R_w} = (0.108)\cdot[(0.188\ \Omega/\text{m})\cdot(1.64\ \text{m})] = 33.3\ \text{m}\Omega$$

$$\overline{P}_w = R_w \cdot \tilde{i}^2 \approx R_w \cdot I_{g\max}^2 = (33.3\text{ m}\Omega)\cdot(16.67\text{ A})^2 = 3.92\text{ W} \Rightarrow \psi = \frac{\overline{P}_w}{\overline{P}_c} = 3.92\text{ W}/3.32\text{ W} = 1.18$$

$$\boxed{\text{2 T130-26 cores with 28 turns of \#22} \times \text{15 round wire, 164 cm}}$$

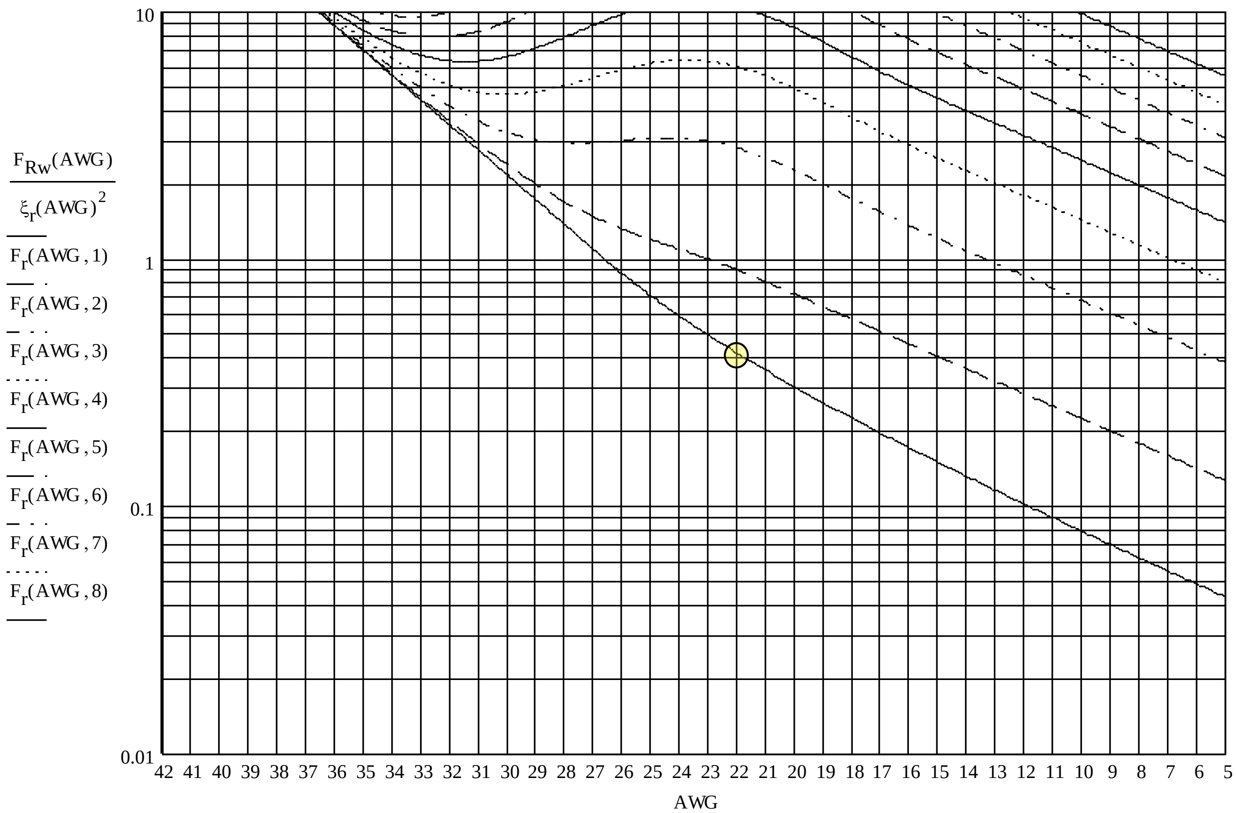

Fig. 2. Eddy-current resistance-ratio F_r at magnetic (switching) frequency f_s = 150 kHz and $R_{\delta r}/l_w$ = 188 mΩ/m for Cu at 80°C. F_r(AWG, M) has winding layers M. The lowest plot F_{rw} is that of a single, isolated wire (no proximity effect). The proximity effect dominates over the skin effect where the plots rise, between ξ_{rv} and ξ_{rp}, for M ≥ 2. F_{rw} for a single isolated #22 wire is highlighted as it's used in calculation of f_{rS} for the primary winding.

References

1. "Designing An Open-Source Power Inverter (Part 1): Goals And Specifications" by Dennis Feucht, How2Power Today, May 2021.
2. "Designing An Open-Source Power Inverter (Part 2): Waveshape Selection" by Dennis Feucht, How2Power Today, September 2021.
3. "Designing An Open-Source Power Inverter (Part 3): Power-Transfer Circuit Options" by Dennis Feucht, How2Power Today, April 2022.
4. "Designing An Open-Source Power Inverter (Part 4): The Optimal Power-Line Waveshape" by Dennis Feucht, How2Power Today, May 2022.
5. "Designing An Open-Source Power Inverter (Part 5): Kilowatt Inverter Circuit Design" by Dennis Feucht, How2Power Today, July 2022.
6. "Designing An Open-Source Power Inverter (Part 6): Kilowatt Inverter Control Circuits" by Dennis Feucht, How2Power Today, August 2022.
7. "Designing An Open-Source Power Inverter (Part 7): Kilowatt Inverter Magnetics" by Dennis Feucht, How2Power Today, September 2022.
8. "Designing An Open-Source Power Inverter (Part 8): Converter Control Power Supply" by Dennis Feucht, How2Power Today, November 2022.
9. "Designing An Open-Source Power Inverter (Part 9): Magnetics For The Converter Control Power Supply" by Dennis Feucht, How2Power Today, December 2022.
10. "Designing An Open-Source Power Inverter (Part 10): Converter Protection Circuits" by Dennis Feucht, How2Power Today, February 2023.
11. "Designing An Open-Source Power Inverter (Part 11): Minimizing Switch Loss In Low-Input-Resistance Converters" by Dennis Feucht, How2Power Today, March 2023.

12. "Designing An Open-Source Power Inverter (Part 12): Sizing The Converter Magnetics" by Dennis Feucht, How2Power Today, May 2023.
13. "Designing An Open-Source Power Inverter (Part 13): The Differential Boost Push-Pull Power-Transfer Circuit" by Dennis Feucht, How2Power Today, June 2023.
14. "Designing An Open-Source Power Inverter (Part 14): Boost Push-Pull Or Buck Bridge?" by Dennis Feucht, How2Power Today, July 2023
15. "Designing An Open-Source Power Inverter (Part 15): Transformer Magnetic Design For the Battery Converter" by Dennis Feucht, How2Power Today, March 2024.
16. "Designing An Open-Source Power Inverter (Part 16): Transformer Winding Design For the Battery Converter—Efficiency Range And Winding Allotment" by Dennis Feucht, How2Power Today, April 2024.
17. "Designing An Open-Source Power Inverter (Part 17): Transformer Winding Design For the Battery Converter—Alternative Configurations" by Dennis Feucht, How2Power Today, May 2024.
18. "Designing An Open-Source Power Inverter (Part 18): Transformer Winding Design For The Battery Converter—Secondary Winding Design" by Dennis Feucht, How2Power Today, July 2024.
19. "Designing An Open-Source Power Inverter (Part 19): Controller Design For The Battery Converter" by Dennis Feucht, How2Power Today, September 2024.
20. "Designing An Open-Source Power Inverter (Part 20): Converter Inductor Magnetic Design" by Dennis Feucht, How2Power Today, October 2024.
21. "How To Optimize Turns For Maximum Inductance With Core Saturation" by Dennis Feucht, How2Power Today, April 2019.
22. "Toroid Window Fill Factor," *Power Magnetics Design Optimization*, D. L. Feucht, Innovatia, 2016, OCT20 revision, pages 121 – 122.
23. "How To Calculate Toroid Winding Length" by Dennis Feucht, How2Power Today, September 2013.
24. "Toroid Turn Length," *Power Magnetics Design Optimization* by D. L. Feucht, Innovatia, 2016, OCT20 revision, pages 116 – 121.
25. "How Twisted Bundles Reduce Eddy-Current Effects In Winding Bundle Design" by Dennis Feucht, How2Power Today, September 2023.

About The Author

Dennis Feucht has been involved in power electronics for 40 years, designing motor-drives and power converters. He has an instrument background from Tektronix, where he designed test and measurement equipment and did research in Tek Labs. He has lately been working on projects in theoretical magnetics and power converter research.

For more on magnetics design, see these How2Power Design Guide search results.